

## Research highlights

Šeila Selimović,<sup>ab</sup> Cole A. DeForest,<sup>c</sup> Mehmet R. Dokmeci<sup>ab</sup> and Ali Khademhosseini<sup>\*abde</sup>

DOI: 10.1039/c2lc90054h

## Predicting localized ligand-based cell signaling

While it is known that spatio-temporally-regulated signaling events play a key role in directing stem cell fate and generating functional tissue, studies that can definitely determine the isolated effects of cell-level organization and autocrine/paracrine signaling *in vivo* have proven elusive. In an effort to understand these highly complex systems, researchers have turned towards *in vitro* models that offer a high level of control over a variety of environmental parameters to assay these essential biological functions. A critical and non-trivial requirement for these platforms is that they recapitulate the spatially- and temporally-diverse aspects of the localized signaling environment.

Recently, Moledina *et al.* have combined computational simulations with experimental microfluidic-based approaches to predict and manipulate the local biological impact of endogenously secreted ligands on a model mouse embryonic stem cell (mESC) culture system.<sup>1</sup> By tuning the unidirectional fluid flow rate over plated cells within a microfluidic device, ligand

presentation to downstream cells was precisely controlled. *In silico* models based on laminar fluid flow predicted the local impact of endogenously secreted activating ligands on transcription signaling as well as the gradient of cell fate determination along the direction of media perfusion.

Stochastic 3D Brownian dynamics were incorporated into a novel computational model for simulating ligand movement within the microfluidic culture system. This approach represents a major advancement over traditional methodologies that utilize deterministic mass transport theories to characterize the ligand movement within perfusion culture; previous methods typically treated cultures as uniform surfaces and were unable to predict the random trajectories of individual ligand molecules upon cellular release. When combined with a deterministic model for cellular expression in response to ligand-mediated signaling,<sup>2</sup> the complete model is able to predict flow-rate dependent effects on cell fate determination (*e.g.*, pluripotency) (Fig. 1a).

To validate the simulated results for flow-mediated control over cell fate, mESCs were seeded within a poly(dimethylsiloxane) (PDMS) microfluidic device generated *via* standard photolithography-based techniques and cultured at saturating levels of exogenous ligand. Upon membrane receptor saturation, the ligand was removed from the inlet media and the cells were exposed to a variety of flow rates (0.011  $\mu\text{L min}^{-1}$  to 1  $\mu\text{L min}^{-1}$ , corresponding to  $Pe = 1$  to 100), which transported the dis- and re-associating ligand downstream. As the ligand was transported throughout the chamber, reversibly binding to cell surfaces along the way, a gradient of cell pluripotency in response to the bound ligand was discerned along the direction

of flow. The observed cell response was in excellent agreement with computational predictions (Fig. 1b).

The proposed methodology, which incorporates both computational and experimental techniques, enables validation of theoretical models over ligand-specific autocrine/paracrine signaling and a more complete understanding of the methods of intercellular communications during disease and development. While initial efforts have focused on just a single cell/ligand pair, the method is generalizable to other ligand-based biological responses and should prove fruitful in better understanding and directing stem cell fate decisions.

## Anisotropic supraparticles generated using microfluidics

Self-assembly of colloids has been shown to lead to the generation of materials with novel properties.<sup>3</sup> These properties arise as a consequence of the order (periodicity) present on the scale of the particle size, but not in the bulk suspension. One example is the formation of

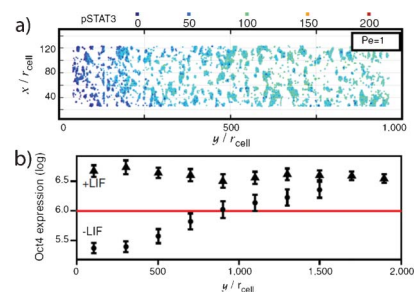


**Fig. 1** A gradient of cell response within the microfluidic channel along the axis of fluid flow was (a) predicted computationally and (b) experimentally validated. Figure reprinted with permission from the National Academy of Science from Moledina *et al.*<sup>1</sup>

<sup>a</sup>Center for Biomedical Engineering, Department of Medicine, Brigham and Women's Hospital, Harvard Medical School, Cambridge, Massachusetts 02139, USA. E-mail: alik@rics.bwh.harvard.edu

<sup>b</sup>Harvard-MIT Division of Health Sciences and Technology, Massachusetts Institute of Technology, Cambridge, Massachusetts 02139, USA

<sup>c</sup>Division of Chemistry and Chemical Engineering, California Institute of Technology, Pasadena, California 91125, USA

<sup>d</sup>Wyss Institute for Biologically Inspired Engineering, Harvard University, Boston, Massachusetts 02115, USA

<sup>e</sup>World Premier International – Advanced Institute for Materials Research (WPI-AIMR), Tohoku University, Sendai 980-8577, Japan

colloidal photonic crystal- (CPC) based materials, which are characterized by the presence of photonic bandgaps as well as their unique light diffraction properties. To better control these characteristics, it is necessary to engineer CPCs with a range of sizes, shapes, and surface functionalities, which has represented a challenging task to date.

Microfluidic methods have proven helpful in generating a variety of CPCs with different properties. Recently, Chen and colleagues have adopted the common microfluidic technique of triphase flow-focusing and generated CPC supraparticles with controllable shape and function. Here, two aqueous liquids, namely a colloidal suspension of polystyrene (PS) particles and a photosensitive solution (trimethylol-propane ethoxylate triacrylate) were co-flowed inside a PDMS capillary. These two solutions showed little diffusive mixing for the duration of the experiment and could therefore be considered immiscible. They were sheared off at a flow junction by a third immiscible fluid, methylsiloxane oil. As described by Yu *et al.*,<sup>4</sup> the sheared off droplets had a Janus shape, with the colloidal suspension being confined to one half of the droplet and the photosensitive solution to the other. Then, the droplets were cross-linked into particles by a UV light source placed downstream above the capillary. Finally, after washing the particles with hexane to remove the oil and subsequent drying, the colloidal PS particles arranged into hexagonal lattices to form hollow CPC supraparticles on the order of 500  $\mu\text{m}$ .

While the co-flow strategy for generation of Janus supraparticles is not new in this work, significant novelty lies in the gained control over exact particle shape. The authors were able to adjust the supraparticle shape by adjusting the interfacial tension between the three immiscible solutions. This was accomplished by adding varying amounts of polyoxyethylene octylphenol ether (*i.e.*, Triton X-100) to the colloidal suspension. As a result, both dumbbell-shaped and spherical core-shell particles were formed. Furthermore, altering the flow rate ratio of the co-flowing solutions enabled an adjustment of the relative sizes of the contributions of the colloidal and photosensitive solutions to the supraparticles. The exact shapes of the

particles were observed by scanning electron microscopy. The size of the particles matched well with the predictions from the Surface Evolver simulations, which utilized information on the interfacial tensions.

Functionality was added to the supraparticles by altering the size of the PS beads. Namely, PS spheres with diameters of 174 nm, 208 nm, and 240 nm resulted in blue, green, and red supraparticles, respectively. This light-reflecting property was attributed to the hexagonal close packing of the PS beads. Thus, the regions of the particles occupied by the crosslinked photosensitive material were correctly predicted to remain dark. Additionally, the particles were rendered supramagnetic by adding iron(III)oxide to the photosensitive solution. Magnetization of the particles at room temperature revealed no hysteresis, indicating that the Janus supraparticles could be reliably manipulated by an external magnetic field. This characteristic was exploited for the generation of rewritable displays. First, individual Janus supraparticles were captured inside hole arrays. Then, upon turning on an alternating magnetic field, a magnetic dipole was induced in each particle, which enabled them to rotate freely. Thus, depending on the direction of the magnetic field, each supraparticle had the PS-bead side turned either toward ("light") or away ("dark") from the observer. In the next step, each supraparticle was assigned its own micromagnetic needle, and could therefore act independently from the other particles. As a result, different patterns on the hole array were produced. The patterns could be rewritten simply by applying the opposite magnetic field.

The ability to control the color as well as the on-off state of the CPC supraparticles in an external magnetic field renders these particles useful for micro-scale displays. The two most important properties in this context are the fact that these displays are rewritable and that this process does not deplete the particles. Thus, the display can be rewritten and turned on and off many times. In the future, this platform could be developed into a full-color display, with blue, red and green CPC supraparticles housed in each hole-array for selective activation.

## Microfluidics for micro-immunohistochemistry

During the process of immunohistochemistry (IHC), cells in a tissue section are analyzed by imaging specific antibody-antigen binding events.<sup>5</sup> Namely, the staining of certain proteins inside the cells is used as an indicator of the amount of protein expression and ultimately of the presence of a disease. The technique of micro-immunohistochemistry ( $\mu\text{IHC}$ ) is IHC conducted on the microscale. The main advantage of analyzing tissue samples on the micrometer scale is the ability to conduct many staining experiments on a relatively small area, without cross-talk between neighboring tissue sections.

Delamarche and colleagues have recently introduced a microfluidic method that enables  $\mu\text{IHC}$ . Lovchik *et al.*<sup>6</sup> developed a simple microfluidic chip containing two channels; one for injection and the other for aspiration of the staining liquids (Fig. 2). The chip was attached vertically to a robotic stage, capable of scanning across the full area of a typical microscope slide ( $1'' \times 3''$ ). This vertical microfluidic probe ( $\nu\text{MFP}$ ) could deliver pL volumes of a liquid sample to specific pre-programmed regions on a substrate. In the context of IHC, this means that different biomolecules could be delivered to certain regions of a tissue sample with high precision. For example, areas as small as 5–10 cells could be patterned with specific antigens, and the programmed patterns could be modified in real-time.

Furthermore, the patterning process could be accomplished at a sample-probe distance of up to 30  $\mu\text{m}$ . This non-contact liquid delivery method could be especially helpful for staining of rare samples, as the samples will not be easily damaged or contaminated during the staining. An additional advantage of the  $\nu\text{MFP}$  was its rhombic shape, with an apex of less than 1  $\text{mm}^2$  in area. This means that the region to be stained could be easily visualized from different angles. Last, the microfluidic probe was reusable and compatible with a variety of organic and water-based solutions.

The utility of the  $\nu\text{MFP}$  was tested in histological analysis of a human thyroid tissue sample. First, an immersion liquid was delivered by the probe to the sample.

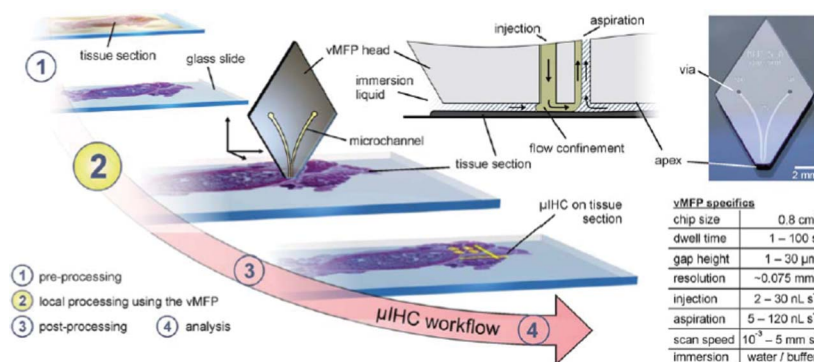


**Fig. 2** Concept of micro-immunohistochemistry using a vertical microfluidic probe (vMFP) and a list of typical experimental parameters. Figure reprinted with permission from the Royal Society of Chemistry from Lovchik *et al.*<sup>6</sup>

Then, the processing liquid was introduced utilizing the same probe at flow rates on the order of a few  $\mu\text{l min}^{-1}$ . The immersion liquid was used to prevent drying artifacts as well as to confine the processing solution. It was shown that the processing liquid (containing fluorescein) remained confined for up to 20 min to an area of  $0.02\text{ mm}^2$ . For comparison, this area was a few times smaller than the area of a biopsied sample and several thousand times smaller than a standard sample excised from a tumor. It was also observed that the present method allowed optimal staining of a sample within 20 s, and that the staining intensity was dependent on the incubation time. This

indicated that the  $\mu\text{IHC}$  method allowed for high density sample processing, both in time and in area. Further validation tests were conducted on cancerous breast tissue samples using 3 different antibodies. The antibodies were used on different regions of the samples, but multiplexed staining was also conducted, in which the same sections were stained with two antibodies. Antigens were only detected in the diseased tissue, but not in the healthy samples.

The  $\mu\text{IHC}$  technique uses 100 times less reagents than standard IHC, allows for high density sample analysis, and enables researchers to quickly adjust the staining protocol for a specific tissue sample and

to test it on nearby tissue samples with similar properties. These characteristics make  $\mu\text{IHC}$  attractive for a variety of biological and pathological applications.

## References

- 1 F. Moledina, *et al.*, *Proc. Natl. Acad. Sci. U. S. A.*, 2012, **109**(9), 3264–3269.
- 2 A. Mahdavi, *et al.*, *PLoS Comput. Biol.*, 2007, **3**(7), e130.
- 3 D. Frenkel and D. J. Wales, *Nat. Mater.*, 2011, **10**, 410–411.
- 4 Z. Yu, *et al.*, *Angew. Chem., Int. Ed.*, 2012, **51**, 2375–2378.
- 5 J. A. Ramos-Vara, *Vet. Pathol.*, 2005, **42**, 405–426.
- 6 R. D. Lovchik, *et al.*, *Lab Chip*, 2012, **12**, 1040–1043.